Structural Role of Tyrosine 98 in Photoactive Yellow Protein: Effects on Fluorescence, Gateway, and Photocycle Recovery[†,‡]

John A. Kyndt,[§,||] Savvas N. Savvides,[||] Samy Memmi,[||] Moonjoo Koh,[⊥] John C. Fitch,[§] Terry E. Meyer,[§] Maarten P. Heyn,[#] Jozef J. Van Beeumen,[||] and Michael A. Cusanovich*[,§]

Department of Biochemistry and Molecular Biophysics, University of Arizona, Tucson, Arizona 85721, Laboratory of Protein Biochemistry and Protein Engineering, Ghent University, K. L. Ledeganckstraat 35, 9000 Ghent, Belgium, Department of Chemistry, Chosun University, Kwangju 501-759, Korea, and Biophysics Group, Department of Physics, Freie Universität Berlin, Arnimallee 14, 14195 Berlin, Germany

Received September 7, 2006; Revised Manuscript Received November 7, 2006

ABSTRACT: We have recently shown that the Y98Q mutant of PYP has a major effect on the photocycle kinetics (∼40 times slower recovery). We have now determined the crystal structure of Y98Q at 2.2 Å resolution to reveal the role of residue Y98 in the PYP photocycle. Although the overall structure is very similar to that of WT, we observed two major effects of the mutation. One obvious consequence is a conformational change of the $\beta4-\beta5$ loop, which includes a repositioning of residue M100. It had previously been shown that the photocycle is slowed by as much as 3 orders of magnitude when residue M100 is substituted or when the conformation is altered as in *Rhodocista centenaria* PYP. To investigate whether the altered photocycle of Y98Q is due to this repositioning of M100 or is caused by an effect unrelated to M100, we determined the dark recovery kinetics of the Y98Q/M100A mutant. We find the recovery kinetics to be very similar to the M100A single mutant kinetics and therefore conclude that the slower recovery kinetics in Y98Q are most likely due to repositioning of M100. In addition, we find that other substitutions at position 98 (Y98W, Y98L, and Y98A) have differing effects on the photocycle recovery, presumably due to a variable distortion of the $\beta4-\beta5$ loop. The second effect of the Y98Q mutation is a repositioning of R52, which is thought to interact with Y98 in WT PYP and now forms new interactions with residues Q99 and Q56. To determine the role of R52, we also characterized an R52A/M100A double mutant and found that the effects on the recovery kinetics (∼2000 slower recovery than WT) are due to unrelated events in the photocycle. Since the Y98Q/M100A recovery kinetics are more similar to those of M100 than R52A/M100A, we conclude that the repositioning of R52, caused by the Y98Q mutation, does not affect the dark state recovery. In addition, it has been proposed that Y98 and P68 are "gateway residues" between which the chromophore must pass during isomerization. We tested the recovery kinetics of mutant P68A and found that, although the gateway may be important for photocycle initiation, its role in recovery to the ground state is minimal.

Photoactive yellow protein (PYP)[1] is a blue light photoreceptor (*1*, *2*), which was originally isolated from *Halorhodospira halophila* (*3*) but has subsequently been found in several purple bacteria and in some nonphototrophs (*4*). More recently, it has also been shown that PYP can be part of multidomain proteins where it forms the N-terminal (∼14 kDa) domain that is followed by a bacteriophytochrome central domain and by either a histidine kinase or diguanylate cyclase enzymatic output domain (*4*−*6*). The photocycle of the prototypic *H. halophila* PYP is complete in less than 1 s (*1*). However, the photocycle can be as much as 2 orders of magnitude faster, as in *Rhodobacter sphaeroides* and *Rhodobacter capsulatus* PYP (*7*, *8*), or 3 orders of magnitude slower, as in *Rhodocista centenaria* Ppr (*5*) and *Thermochromatium tepidum* Ppd (*6*). Considerable effort has been expended to determine how the protein modulates the photocycle, not only to understand the fundamental mechanism of signal transfer but also to design PYP mutants with long-lived intermediates that could function in optical switching devices (*9*).

In the prototypic *H. halophila* PYP, the photocycle can be initiated by a laser flash at 450 nm, which is near the wavelength maximum of 446 nm, that results in a *trans* to *cis* isomerization of the chromophore, *p*-hydroxycinnamic acid. In the initial steps of the photocycle, it is thought that the chromophore undergoes concerted motions with residues P68 and Y98 which form a gateway with ratchet-like

[†] This work was supported by a grant from the NIH, GM66146.

[‡] The coordinates and structure factors for Y98Q PYP are available via the Protein Data Bank (www.rcsb.org) with accession code 2I9V.

* To whom correspondence should be addressed. Tel: (520) 621-7533. Fax: (520) 621-6603. E-mail: cusanovi@u.arizona.edu.

[§] University of Arizona.

[||] Ghent University.

[⊥] Chosun University.

[#] Freie Universität Berlin.

[1] Abbreviations: PAS, acronym formed of the names of the first three proteins recognized as sharing this sensor motif (*p*eriodic clock protein of *Drosophila*, *a*ryl hydrocarbon receptor nuclear translocator of vertebrates, *s*ingle-minded protein of *Drosophila*); PYP, photoactive yellow protein; WT, wild type; Ppr, PYP−phytochrome related; Ppd, PYP−phytochrome−diguanylate cyclase.

10.1021/bi061867y CCC: $37.00
Published on Web 01/02/2007

properties through which the carbonyl group of the chromophore needs to pass to initiate the photocycle (*10*). Concomitant with the chromophore isomerization is the conversion of the dark-adapted state P into I_0 (1.9 ps) and subsequently into $I_0^{\ddagger}$ (220 ps), both absorbing at 510 nm (*11*−*13*). $I_0^{\ddagger}$ decays into the red-shifted I_1 intermediate in about 3 ns (λ_{max} = 465 nm). In ~500 μs, I_1 decays to I_1', which has the ionized chromophore exposed to the solvent (*14*). Fast protonation by the solvent results in the blue-shifted I_2 (λ_{max} = 350 nm). Recently, evidence was provided for an I_1'/I_2 equilibrium in the E46Q *H. halophila* PYP mutant and for WT PYP (*14*), and a similar pH-dependent equilibrium was found in the *T. tepidum* PYP photocycle (*6*). A major conformational change of the protein, in about 1.5 ms, forms the I_2' intermediate (*13*, *15*). The I_2 and I_2' intermediates are in equilibrium (*16*), and this equilibrium is pH dependent with a pK_a of 6.4 (*17*, *18*). The return to the dark-adapted state occurs with a lifetime of about 160 ms. Since the I_2' intermediate is the longest lived intermediate and undergoes a major conformational change, it is generally believed to be the signaling state that interacts with an unknown partner in the case of *H. halophila* PYP.

The three-dimensional structure of *H. halophila* PYP is composed of a central, twisted, six-stranded antiparallel β-sheet, which is flanked on both sides by loops and helices (*19*). There are hydrophobic cores on each side of the central β-sheet with the chromophore binding in the major hydrophobic groove. This fold is known as the PAS fold, and PYP is the prototype of this structural motif. PAS domains are found in a large variety of sensory proteins that respond to a diverse range of compounds and stimuli (for reviews see refs *2* and *20*). A comparison of the three-dimensional structure of the PYP ground state to that of one of the photocycle intermediates (presumably I_2; *21*) indicates that the side chain of R52 (in loop $\alpha3-\alpha4$) blocks access to the solvent and must move out of the way of the chromophore during isomerization. The X-ray structure suggests that R52 forms a hydrogen bond with the backbone carbonyl of Y98 (*19*), while the NMR solution structure suggests an interaction between R52 and the Y98 ring structure (*22*). Once the chromophore is in the *cis* conformation in the I_2 state, the hydroxyl hydrogen bonds with E46 and Y42 are broken and a new hydrogen bond to the side chain of R52 is formed (*21*). We have found that the R52A mutant slows recovery by 6-fold and reduces protein stability, which underscores its importance (*23*). Another residue in close proximity to the chromophore is M100, which is located on the $\beta4-\beta5$ loop. It was found that the rate of recovery was reduced by 3 orders of magnitude in the M100A mutant (*24*). A similar effect on recovery was observed with M100K, M100E, and M100L mutants (*25*). It is therefore believed that M100 catalyzes the *cis*−*trans* isomerization of the chromophore in the ground state recovery. Photoreversal studies with M100A show indeed that reisomerization of the chromophore is the rate-limiting step in the recovery (*24*). The structure of the PYP domain of *R. centenaria* Ppr was recently solved and showed a novel conformation of the $\beta4-\beta5$ loop (*26*). *R. centenaria* PYP and the *T. tepidum* PYP domain are the only two PYPs that have a Y98F substitution. The crystal structure shows that, at least in *R. centenaria* PYP, F98 is oriented toward the protein interior as opposed to Y98 in *H. halophila* PYP which is facing outward. This repositions M100 in a way that it is inaccessible for interaction with the chromophore and provides a possible explanation for the slower recovery kinetics of the *R. centenaria* PYP domain (*26*). On the other hand, we have recently shown that the Y98F mutation in *H. halophila* PYP has no significant effect on the photocycle recovery kinetics (*27*). A Y98Q mutation, however, has a major effect on the photocycle kinetics. We observed a 3−4-fold decrease in the rise of I_2 and I_2', a major decrease in recovery rate to the ground state (~40 fold slower than WT), and a dramatic shift in the I_1/I_2 equilibrium toward I_1 (*27*). This equilibrium was shown to be strongly pH dependent with a pK_a of 6.3. In addition, we observed a significant salt effect on the photocycle kinetics and proposed that the I_2 to I_2' transition is controlled by an ionic lock between the β-scaffold and the N-terminal cap (*27*). To gain insight into the mechanism underlying the effects of the Y98Q mutation, we have determined the structure of the Y98Q mutant and characterized additional substitutions at position 98. On the basis of the results of that structure, we also prepared two double mutants to study the effect of residues M100 and R52 on the recovery kinetics of the PYP photocycle and investigated the role of the second "gateway residue" P68 using a P68A mutant.

MATERIALS AND METHODS

Protein Production and Purification. H. halophila holo-PYP was produced by the use of the biosynthetic enzymes TAL and pCL and subsequently purified from *E. coli* BL21-(DE3) as described (*28*). The mutagenesis was performed as described (*8*).

Crystallization, X-ray Data Collection, and Structure Determination. Single crystals of Y98Q PYP suitable for data collection were obtained by microseeding techniques starting with grossly twinned crystals grown by the hanging drop vapor diffusion method from droplets containing 2 μL of protein sample (10 mg/mL Y98Q PYP in 5 mM Tris-HCl, pH 7.5) and 2 μL of reservoir solution (3.2 M ammonium sulfate and 20 mM sodium phosphate, pH 5.9). Crystalline seeds were prepared by pulverizing twinned crystals in 50 μL of stabilization buffer (3.2 M ammonium sulfate and 20 mM sodium phosphate, pH 5.9). Aliquots (0.5 μL) of the seed suspension (diluted 1:100 in stabilization buffer) were introduced into a series of fresh hanging drops (containing 4 μL of protein sample and 4 μL of reservoir solution) that had been equilibrated for 24 h over reservoirs containing 3 M ammonium sulfate and 20 mM sodium phosphate, pH 5.4−6.2. Single crystals with bipyramidal morphology grew after 1 week to a final size of 0.150 mm × 0.150 mm × 0.100 mm.

To prepare crystals for data collection under cryogenic conditions (100 K), crystals were flash-cooled by plunging them directly from their native drops into liquid nitrogen. A series of cryocooling conditions using a variety of cryoprotecting reagents such as glycerol, sucrose, PEG 400, and paratone indicated that only crystals flash-cooled by plunging them directly from their native drops into liquid nitrogen produced diffraction of acceptable quality. Crystals of Y98Q PYP belong to space group *R*3 with unit cell parameters $a = b = 86.75$ Å, $c = 56.92$ Å, $\alpha = \beta = 90°$, and $\gamma = 120°$. A complete data set was collected to 2.2 Å resolution using synchrotron radiation at beamline X13 of the EMBL Outsta-

Table 1: Data Collection and Refinement for *H. halophila* Y98Q PYP

data collection	
space group	*R*3
unit cell	$a = b = 86.75$ Å, $c = 56.92$ Å, $\alpha = \beta = 90°$, $\gamma = 120°$
source, wavelength (Å)	DESY/X13, 0.8067
resolution (Å)	30−2.2
reflections (total/unique)	46637/8065
completeness (%)	100 (100)
R_{merge}[a] (%)	8.6 (33.1)
$I/\sigma(I)$	22.9 (5.8)
refinement	
PDB code	2I9V
resolution (Å)	30−2.2
$\|F\|/\sigma(\|F\|)$	0
no. of reflections (working set/ test set)	6977/822
molecules per asymmetric unit	1
protein atoms	969
chromophore atoms	11
water molecules	71
R_{cryst}, R_{free}	0.199, 0.241
rms deviations	
bonds (Å)	0.006
angles (deg)	1.2
B values (Å2) (main chain/ side chain)	1.4/1.9

[a] $R_{merge} = \sum_h\sum_i|I(h,i) - \langle I(h)\rangle|/\sum_h\sum_i I(h,i)$, where $I(h,i)$ is the intensity of the *i*th measurement of reflection *h* and $\langle I(h)\rangle$ is the average value over multiple measurements. Values in parentheses correspond to values in the highest resolution shell (2.25−2.2 Å).

tion in Hamburg, Germany (Table 1). Data processing was carried out using the programs DENZO and SCALEPACK (*29*). Intensities were converted into structure factor amplitudes using the program TRUNCATE from the CCP4 suite (Collaborative Computational Project, Number 4, 1994).

The structure of Y98Q PYP was determined by molecular replacement using maximum likelihood methods implemented in PHASER, version 1.2 (*30*), using the atomic coordinates of the WT PYP in its dark state (PDB entry 2PHY) after substituting Y98 by alanine and stripping the model of all water molecules and its chromophore.

The correctness of the structure solution was assessed from the quality of the electron density for the missing chromophore, the glutamine side chain at position 98, and other unique structural features. Rounds of model building were subsequently alternated with crystallographic refinement employing simulated annealing, conjugate gradient minimization, and individual *B*-factor refinement using a maximum likelihood target function, as implemented in CNS (*31*) (Table 1). The stereochemical correctness of the final model was assessed with the program MOLPROBITY (*32*). The structure has excellent stereochemistry, with 94% of all ϕ/ψ angles belonging in the favored regions of the Ramachandran plot and no outliers.

Mass Spectrometry. All of the mutants were checked for the correct mutation by mass spectrometry. These experiments were performed at the Chemistry Department mass spectrometry facility of the University of Arizona. Samples (10 μM) were submitted in 5 mM Tris-HCl and were analyzed with ESI-MS, preceded by an HPLC separation.

UV−Vis and Time-Resolved Laser Spectroscopy. Absorption spectra were obtained with a CARY 300 spectrophotometer. All studies were carried out in a universal buffer (2 mM CAPS, CHES, TAPS, HEPES, MES, sodium citrate, 1 mM PIPES), unless otherwise indicated. In the steady-state recovery experiments of the M100 single and double mutants, the protein was first bleached by 40 s exposure to a tungsten lamp (60 W), and the subsequent recovery was measured in the dark in the CARY spectrophotometer. A 410 nm cutoff filter was used to excite only the 446 nm form. This eliminated photoreversal and increased the intensity of the bleach. Absorbance changes were measured over a 40−120 min time range, and the kinetic data were fit using OLIS software (Bogart, GA).

The laser flash photolysis apparatus and data analysis protocol for the fast kinetics of WT and Y98 single mutants were as described previously (*1*, *33*). Samples with an A_{446} of about 0.3 in universal buffer were used.

Fluorescence Spectroscopy. All of the samples for the fluorescence measurements were in 20 mM Tris-HCl (pH 7.5) and had an A_{446} of about 1.3. Samples were measured on a PC1 photon counting spectrofluorometer (ISS, Champaign, IL), and the data were analyzed with the VINCI software.

RESULTS

Crystal Structure of Y98Q. The structure of Y98Q PYP largely maintains the structural elements of the dark state WT structure (*19*) but reveals significant rearrangements in the $\beta4-\beta5$ loop (residues 98−101), the $\alpha1-\alpha2$ loop (residues 17−22), the $\beta5-\beta6$ loop (residues 112−115), and the N-terminus (residues 1−3) (Figure 1A). The latter three regions have the largest temperature factors in WT protein; thus it is not surprising that they adopt a different conformation in mutant Y98Q, especially considering that the two proteins crystallize in different space groups. Interestingly, Y98Q PYP crystallizes in a rhombohedral lattice (*R*3) instead of the primitive-hexagonal lattices observed for all other variants crystallized to date. The structures of Y98Q and WT PYP can be overlaid with an rmsd of 0.86 Å for all Cα atoms and with an rmsd of 0.42 Å when the $\beta4-\beta5$ loop, the $\alpha1-\alpha2$ loop, the $\beta5-\beta6$ loop, and the first three residues at the N-terminus are excluded from the calculations. Analysis of crystal contacts in Y98Q PYP reveals that the $\beta4-\beta5$ loop is involved in a new set of interactions, with the N-terminus of a symmetry-related molecule instead of with C-terminal residues in the WT structure. Nevertheless, this loop is very well ordered in the Y98Q structure (this was also the case in the WT structure; *19*), which allowed us to unambiguously model it in the electron density. Q98 in Y98Q PYP has moved outward compared to Y98 in WT, whereas Q99 has moved inward to compensate for the absence of Y98 (Figure 1B). The chromophore remains in the *trans* ground state position and is only slightly repositioned. It shifted over ~0.4 Å and has rotated slightly over ~12°. The hydrogen bond interactions with the side chains of residues Y42 and E46, which are important for spectral tuning, remain intact. The distance to the phenolic oxygen is 2.43 Å for Y42 and 2.46 Å for E46, which is in agreement with the WT values (<2.6 Å) for these unusually short hydrogen bonds (*34*). As a consequence of the $\beta4-\beta5$ loop repositioning, residue M100 has collapsed toward the center by about 1.5 Å, resulting in the S_δ atom being closer to the chromophore (Figure 1C).

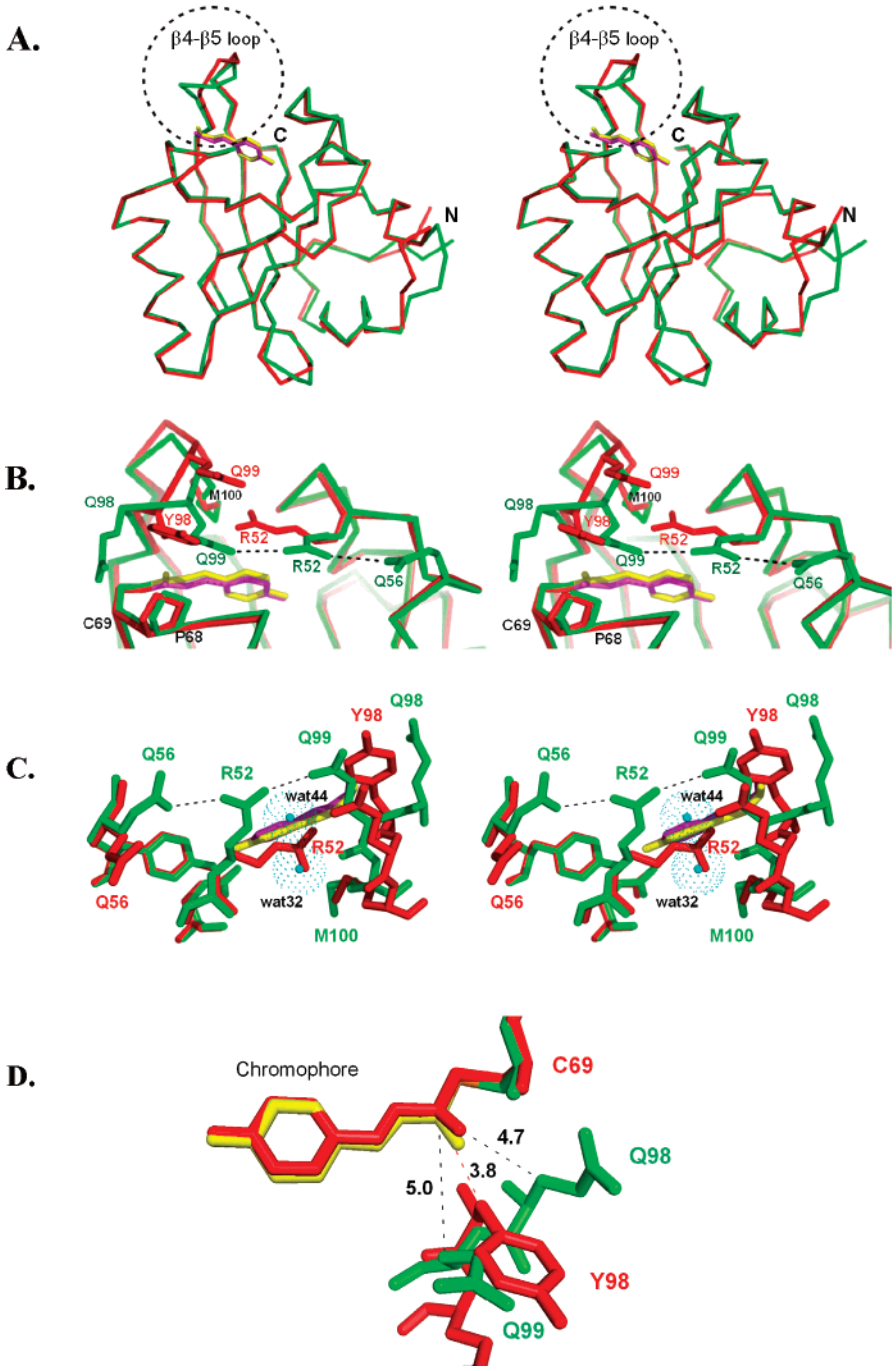

FIGURE 1: Crystal structure of Y98Q PYP. This figure was prepared with the program PyMOL, version 0.98 (www.pymol.org). (A) Stereoview of a superposition of the backbone of Y98Q (green and yellow) with WT PYP (red and purple). The main conformational changes were located at the $\beta4-\beta5$ loop (top circled), and minor changes were observed in the $\alpha1-\alpha2$ loop (front far right), the $\beta5-\beta6$ loop (bottom), and the N-terminus (far right, rear). Structural overlays were carried out using the program SEQUIOA, version 0.9.9 (*46*). (B) Stereoview of the structure in the vicinity of the $\beta4-\beta5$ loop highlighting the conformational changes that have taken place in Y98Q. WT residues are labeled in red and Y98Q residues in green. (C) Detailed stereoview of the chromophore region. View from the solvent side, showing the two water molecules (wat32 and wat44) that fill in the gap after R52 repositioning and the new interaction of R52 with Q56 and Q99. The WT chromophore configuration is shown in red and purple, while the Y98Q chromophore is presented in green and yellow. The repositioning of M100 can be seen on the bottom. (D) Detailed view of the gateway in WT (red) and Y98Q (green and yellow). Distances (in Å) are indicated in black. The chromophore carbonyl oxygen needs to flip about 180° (in the direction of Y98) to form the *cis* isomer in the early photocycle events. Mutating Y98 opens the gateway and allows the chromophore (yellow) to obtain a more planar conformation.

The distance between C4 of the chromophore ring and the S_δ of M100 has shortened from 4.9 to 4.2 Å, while the distance between the C7−C8 double bond of the chromophore and the S_δ of M100 has changed from 4.6 to 4.2 Å in Y98Q PYP. Finally, we observe a dramatic conformational change in the side chain of R52. Residue R52 is known to shield the chromophore from solvent and undergoes a dramatic relocation of ~10 Å toward the solvent when the chromophore moves out into solution during the photocycle (*21*). In the Y98Q structure, R52 has rotated about 120° around its $C\beta-C\gamma$ bond, thereby replacing the interactions with the backbone carbonyl oxygen atoms of residues Y98 and T50 by interactions with the side chains of two new partners, Q99 and Q56 (Figure 1C). Q56 itself has reposi-

tioned its side chain over ~4 Å to make this interaction possible. The gap left behind by R52 is filled in by two water molecules (wat32 and wat44). This brings these two solvent molecules in close proximity to the ring of the chromophore (closest distance is 3.63 Å to wat44).

It has been proposed that concerted motions of residues Y98 and P68 result in the opening of the "gateway" leading to the initiation of the photocycle (*10*). During a 180° flip of the chromophore's thioester linkage, the thioester oxygen atom needs to move through the gateway formed between C9 of the chromophore and the *pro-R* Cβ hydrogen of Y98. Figure 1D shows that the repositioning of residue 98 in the mutant structure opens this gateway by almost 1 Å based on distances measured from the Cβ position of Y98 to the chromophore C9 atom. Although Q99 has now moved inward to emulate the position of Y98, the gateway is not restored since the distance between the Cβ of Q99 and the chromophore C9 remains relatively large (5 Å). P68 has only slightly repositioned in the Y98Q structure (by 0.3 Å). Taken together, our structural analysis reveals an enlargement of the opening capable of altering the picosecond kinetics. It is also visible from Figure 1D that the movement of the Cβ of Y98 has allowed the chromophore C9 carbonyl group to reposition over ~0.6 Å, while the rest of the chromophore has taken on a more planar conformation.

UV−Vis and Fluorescence Spectroscopy. To investigate whether the changes in the side chain at position 98 have an effect on the spectral properties of PYP, we investigated the UV−vis absorbance and fluorescence of several Y98 substitutions. WT PYP shows a low level of fluorescence (quantum yield of about 0.2%; *35*). The fluorescence excitation spectrum (with fluorescence emission at 499 nm) and the emission spectrum (with fluorescence excitation at 446 nm) of the Y98Q mutant are given in Figure 2A (red line). WT fluorescence excitation and emission were also measured as a control and are included in Figure 2A (black line). Although the absorption maximum is very similar in Y98Q and WT PYP (see Figure 2B; 447 nm for Y98Q vs 446 nm for WT), the emission maximum of WT PYP at 495 nm is slightly shifted to 499 nm in the Y98Q mutant. In addition, WT PYP and Y98Q show a significant difference in intensity of fluorescence excitation and emission (~3-fold). The samples were adjusted to the same absorption at 446 nm. To determine the extent to which fluorescence was dependent on the nature of the substituting residue, we also investigated the fluorescence of Y98A and Y98F mutants. We found that the Y98A mutation also increases the fluorescence excitation and fluorescence emission by a factor of 3 compared to WT PYP (green line in Figure 2A). The fluorescence emission maximum has shifted even further in this mutant, to 502 nm. In contrast, the fluorescence excitation and emission intensity of the Y98F mutant was virtually identical to the WT values (yellow line in Figure 2). We prepared the P68A mutant and found that it has an even greater effect on fluorescence excitation and emission (~4-fold compared to WT; blue line in Figure 2). The emission wavelength has also shifted toward 502 nm, similar to the Y98A mutant. All samples had an absorbance of 1.3 at the excitation wavelength, to ensure spectra of high signal-to-noise ratio. Under these conditions, the emission and excitation spectra are not linear in the concentration ("inner filter effect"; see, e.g., ref *36*). Since the absorbances are

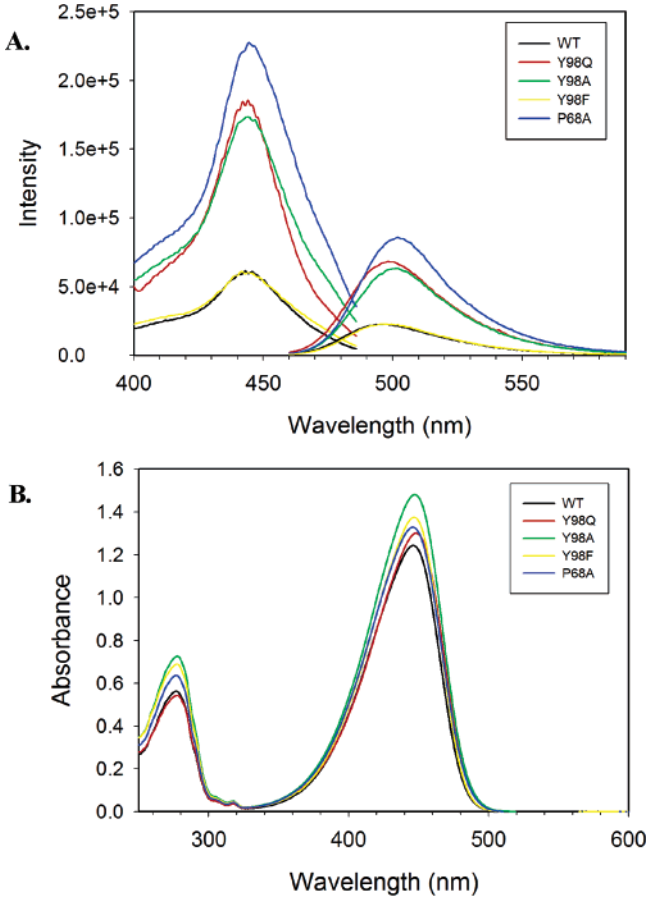

FIGURE 2: (A) Fluorescence excitation (with fluorescence emission at 499 nm) and emission spectra (with fluorescence excitation at 446 nm) of WT PYP, Y98Q, Y98F, Y98A, and P68A. (B) UV−vis spectra of the samples used in (A). All spectra were taken in 20 mM Tris-HCl (pH 7.5).

the same, however, the inner filter effects are also the same for all samples allowing a comparison. The observation that Y98Q, Y98A, and P68A have 3−4-fold larger amplitudes of their emission and excitation spectra than WT, is thus due to the larger fluorescence quantum yields of these mutants.

Recovery Kinetics of Y98 Mutants. It was shown recently that Y98F has similar recovery (I_2' to ground state transition) kinetics as WT, while the Y98Q recovery rate constant is decreased about 40-fold (*27*). To determine to what degree the recovery is influenced by the side chain at position 98, we compared the rate constant for recovery and the influence of pH on recovery in the following Y98 mutants: Y98Q, Y98A, Y98W, and Y98L. The absorption maxima of these were 447 nm for the first two and 446 nm for the latter two (see Figure 2B), and the photocycle could be initiated in all cases with a 450 nm laser flash. We had already shown that the pH dependence of Y98Q recovery has a bell-shaped curve with a maximum at pH 8.0 that could be fit with pK_a values of 6.3 and 9.5 (*27*). As shown in Figure 3, the rate of recovery of all the other Y98 mutants also has a bell-shaped pH dependence similar to WT PYP (*23*). The data for Y98Q is included in Figure 3 for comparison. The dependencies for all of the other Y98 mutants could be fit with pK_a values of about 6.5 and 9.4, similar to those for Y98Q (*27*) and WT (6.4 and 9.4) (*23*). The maximum recovery rate constant is at pH ~8 for all mutants; however, there are significant

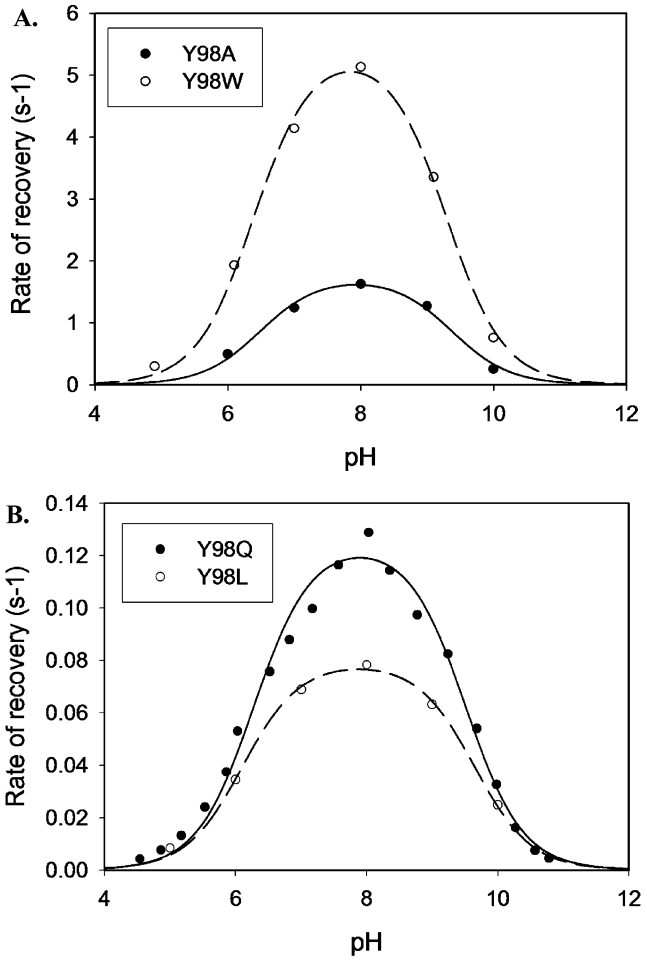

FIGURE 3: pH profile of the kinetics of recovery ($I_2' \rightarrow P$) of the Y98 mutants (A) Y98A and Y98W and (B) Y98Q and Y98L. Note the different scales on the *Y* axes in (A) and (B).

differences in the rate constant for recovery (Table 2). Mutants Y98W, Y98F, and WT have essentially identical pH profiles and kinetics. However, as compared to WT, Y98Q recovery is ~40 times slower (*27*), Y98L ~70 times slower, and Y98A ~3-fold slower. To determine whether the difference in recovery kinetics could correlate with a difference in stability, we examined the overall stability of each of the mutants with calorimetry and acid denaturation but found little variation among them ($T_m \sim 75-80$ °C as compared to 82 °C for WT and the pK_a for acid denaturation ~3.0−3.4 vs 2.8 for WT; data not shown). Morishita et al. (*37*) also prepared the Y98A mutant and observed a 4-fold slower recovery and a denaturation temperature of 81 °C, which is very similar to our findings.

Since P68A had similar effects on the intensity of fluorescence as the Y98 mutations, we also determined the effect of the P68A substitution on the rate constant for recovery, which was only 2-fold slower compared to WT PYP (3.2 vs 6.1 s^{-1} for WT) and had a similar pH dependence (data not shown).

Table 2: Recovery Rate Constants for PYP at pH 8.0

	rate constant (s^{-1})		rate constant (s^{-1})
WT	6.1	P68A	3.2
Y98W	5.1	R52A	1.2
Y98F	4.8	M100A	3.0×10^{-3}
Y98A	1.6	Y98Q/M100A	2.9×10^{-3}
Y98Q	0.13	R52A/M100A	1.6×10^{-3}
Y98L	0.078		

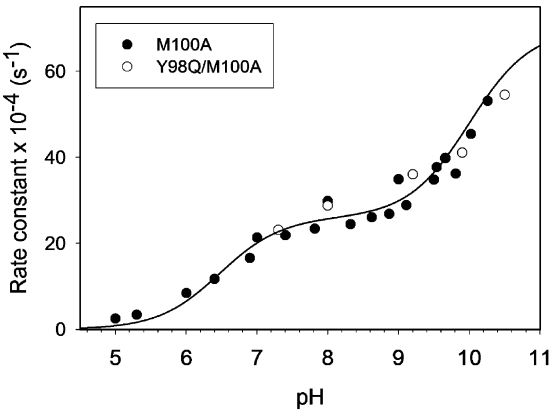

FIGURE 4: pH profile of the kinetics of recovery of M100A (closed circles) and Y98Q/M100A (open circles). The M100A data were fit with a 2 pK_a curve [pK_a(1) = 6.5, $n_1 = 1$; pK_a(2) = 10, $n_2 = 1$].

Kinetics of the Y98Q/M100A Double Mutant. Since the X-ray structure of Y98Q showed a significant repositioning of residue M100, we prepared the Y98Q/M100A double mutant and analyzed its kinetics to determine whether the decreased rate constant for recovery is linked to the M100 repositioning. It is noteworthy that the yield of this mutant was significantly lower than that of the single mutants, suggesting a decreased stability of the protein. However, we were able to purify sufficient protein to measure the recovery kinetics. The recovery kinetics of Y98Q/M100A at pH 8.0 was very similar to the recovery of the M100A single mutant (Table 2 and compare to ref *24*). This indicates that the two mutations do not have an additive effect (which would result in a 40-fold slower recovery of the double mutant compared to M100A). M100A has a sigmoidal pH dependence (in the pH range 5−9) with a pK_a of 7 (*24*). Thus, we determined the pH dependence of the Y98Q/M100A double mutant in the range of pH 7−10.5. Note that the double mutant was unstable above pH 10.5. Figure 4 gives the pH profile of the recovery rates of both the single M100A mutant and the double mutant. While reinvestigating the pH dependence of the M100A recovery rate, it became clear that, upon enlarging the pH range to the upper limit of stability, ~10.5, the pH dependence of the single mutant is best fitted with two pK_a values (pK_1 = 6.5; pK_2 = 10.0). There is a clear overlap between the two curves in Figure 4, indicating that the effects of the double mutant on the recovery are very similar to those of the M100A single mutant.

Kinetics of the R52A/M100A Mutant. The structure of Y98Q also showed a significant repositioning of R52. It has been shown that an R52A mutation of PYP has a similar pH dependence for recovery as WT and is governed by similar pK_a values, but the optimum rate constant at pH 8 is about 5−6 times slower (*23*). To further investigate the role of R52A, we designed an R52A/M100A mutant. The absorption maximum of the R52A/M100A double mutant was like WT, but the kinetics differ markedly. The recovery rate of the R52A/M100A double mutant is $\sim 1.5 \times 10^{-3}$ s^{-1} at pH 8.0. Thus, it appears that the R52A mutation has an additional effect, that is, a 2-fold slower recovery as opposed to the M100A mutant (Table 2). The pH profile of the R52A/M100A mutant is shown in Figure 5. The R52A/M100A

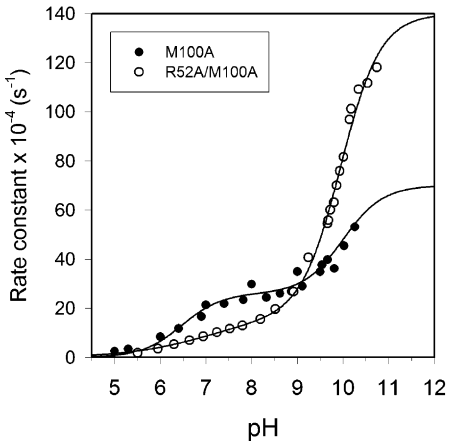

FIGURE 5: pH profile of the kinetics of recovery of M100A (closed circles) and R52A/M100A (open circles). The M100A data are the same as in Figure 5, and R52A/M100A data were fit with a 3 pK_a curve [pK_a(1) = 6.1, n_1 = 1; pK_a(2) = 7.6, n_2 = 1; pK_a(3) = 10, n_3 = 1].

mutant is similar, but not identical, to M100A, with a sigmoidal pH dependence which can be fit with at least two pK_a values, 7.0 (n = 0.5) and 10.0 (n = 1). These pK_a values are similar to the values for M100A, which was expected since the R52A mutant did not change the pH dependence of the recovery reaction compared to WT. However, an n-value significantly less than 1 implies that the situation is more complex. Thus, we fit the R52A/M100A data using three pK_a values, 6.1, 7.6, and 10.0, all constrained to n = 1 (Figure 5). It is notable that as the pH is raised above 9, the double mutant recovery rate constants become significantly larger than for M100A by a factor of 2 (Figure 5).

DISCUSSION

We have determined the crystal structure of the Y98Q mutant of *H. halophila* PYP to 2.2 Å resolution, and on the basis of the resulting structural insights, we have carried out additional site-directed mutagenesis, kinetic studies, and fluorescence spectroscopy to rationalize the role of residues suspected to affect the photocycle.

The overall structure of the Y98Q mutant is very similar to the WT ground state structure (*19*). Four regions are clearly repositioned in the mutant compared to WT: the N-terminal three residues, the α1−α2 loop, the β5−β6 loop, and the β4−β5 loop. The first three regions have the largest temperature factors both in WT and in the mutant protein and were also the most flexible regions in the solution NMR structure (*19*, *22*). In a previous publication, we described the effect of salt on the photocycle of Y98Q and suggested that the formation of I_2' involves the opening of an "ionic lock" formed by residues K110 (on strand β5) and E12 (on the N-terminal domain) (*27*). Although there are rearrangements in the α1−α2 loop and the β5−β6 loop in the Y98Q mutant structure, it still shows a possible linkage between K110 and E12, similar to WT PYP. This is in agreement with the salt effect observed earlier (*27*). The chromophore in Y98Q is still in the *trans* conformation and shows only a slight rearrangement, while its interactions with E46 and Y42 are maintained. On the other hand, the repositioning of the β4−β5 loop is expected to be significant for the photocycle since it contains M100, a residue that has been proposed to catalyze the reisomerization of the chromophore during recovery of PYP (*24*). M100 has moved toward the center of the protein by ∼1.5 Å. However, it is important to note that this distance is measured in the ground state and might not reflect the actual distances in the signaling state I_2' for which no structural data are available. It is known that the largest conformational change of the protein occurs during the I_2 to I_2' transition and that the chromophore ring moves out toward the solvent during signaling state formation (*21*); thus a more inward-oriented M100 might actually increase the distance between the S_δ of M100 and the chromophore in the I_2' state. The large decrease in the rate constant for recovery of Y98Q following bleaching (40-fold) could be unrelated to the positioning of M100. However, the kinetics and pH dependence of the Y98Q/M100A mutant were virtually identical to those of the M100A single mutant. Thus the β4−β5 loop in Y98Q positions M100 so that it cannot efficiently catalyze reisomerization, basically a similar consequence on recovery kinetics that results from the M100A mutation.

Whereas the Y98Q mutation slowed the recovery significantly, the Y98F mutation does not affect the recovery kinetics (*27*). We have now analyzed several other point mutations of Y98. On the basis of the recovery kinetics, we can divide the mutants into three groups: Y98F and Y98W have similar recovery kinetics to WT PYP, indicating that an aromatic residue is necessary to maintain the WT fold of the β4−β5 loop, as already suggested in ref *27*. Y98A has about 3−4-fold slower recovery kinetics than WT PYP (also ref *37*), and Y98Q and Y98L have 40−70-fold slower recovery kinetics. In addition, we found that there is a difference in the fluorescence intensity and emission wavelength of the various Y98 mutants. The increase in fluorescence and the slower rate of recovery of the different Y98 mutants appear to be correlated. Y98F has a low fluorescence intensity, comparable to WT PYP, while Y98A and Y98Q show about 3-fold higher fluorescence emission and excitation. An increase in fluorescence of even greater magnitude (10-fold higher than WT) was reported for the Y42F mutant (*38*), and it has been suggested that bowing of the chromophore could be responsible for this increase in fluorescence (*10*). In the high-resolution structure (0.85 Å) of WT PYP it was observed that the chromophore does not have a flat geometry but is slightly arched out of the plane of its aromatic system (∼0.25 Å), whereas in the Y42F mutant structure, the chromophore is bowed in the opposite direction (*10*). The Y98Q structure, however, shows that the hydrogen bond with Y42 is still present, while the chromophore has a more planar geometry, whereby the π-bonding orbitals of the ring structure are expected to conjugate maximally with those from the C7−C8 double bond. The fact that the configuration of the chromophore in Y98Q is in between the different arched configurations of WT and Y42F and that the fluorescence in the Y98 mutants is intermediate (3-fold increase in Y98Q versus 10-fold increase in Y42F) is consistent with chromophore bowing regulating chromophore fluorescence. An unrelated study of the kindling fluorescent protein (KFP) from *Anemonia sulcata* has shown a similar relationship between the suppression of fluorescence and a substantial distortion from planarity of the chromophore (*39*). Both the PYP and KFP studies show that a change in planarity of the chromophore and concomitant change in

fluorescence are consistent with a change in the direct protein environment of the chromophore.

Integrating the kinetic studies, structural data, and fluorescence results, we conclude that the Y98 mutations result in differing extents of distortion of the $\beta4-\beta5$ loop, with Y98F and Y98W having minimal effects on the loop, Y98A resulting in a small perturbation, and Y98Q and Y98L resulting in very large perturbations which significantly inhibit dark reisomerization. Thus, PYP requires an aromatic residue at position 98 to maintain the conformation of the $\beta4-\beta5$ loop, including M100, to sustain WT recovery kinetics. In WT PYP, residue M100 is positioned at an optimal distance from the chromophore to catalyze isomerization during recovery. Changes in that distance will alter the efficiency of reisomerization catalysis and will be reflected in the kinetics of recovery. In addition, we had speculated in our previous study on Y98Q and Y98F (*27*) that there is a need for an aromatic residue at position 98 to stabilize the I_2 structure. During I_2 formation, the chromophore ring might interact with the ring of Y98 through $\pi-\pi$ stacking (*21*, *27*). The lack of an aromatic residue at position 98 in Y98Q, Y98L, and Y98A makes the presumed $\pi-\pi$ stacking with the chromophore ring impossible and could shift the I_1/I_2 equilibrium toward I_1, in agreement with the shift in this equilibrium we observed earlier for Y98Q (*27*). The finding that Y98A recovery kinetics are close to wild-type might indicate that the $\pi-\pi$ interaction is replaced by an interaction between a methyl group and the aromatic ring. Such weak CH$-\pi$ interactions have been shown to be important for the PYP photocycle (*40*). However, the slow photocycle of Y98Q and Y98L excludes the possibility of these CH$-\pi$ interactions as significant factors in this case. Because Y98Q, Y98L, and Y98A all have different kinetics of recovery, it is likely that they make specific interactions in I_2 that change the orientation of M100 to an even greater extent than in the resting state. Further analysis will be necessary to identify the nature of these interactions.

Another significant observation from the Y98Q structure is a repositioning of R52. The R52 side chain has rotated about 120° around the C$\beta-$Cγ bond and replaced the interactions of its guanidinium group with the backbone carbonyl oxygen atoms of residues Y98 and T50 with new interactions with the side chain carbonyl oxygen atoms of residues Q99 and Q56. We had suggested in our previous publication that there might be a stabilization of the $\alpha3-\alpha4$ and the $\beta4-\beta5$ loops through an interaction between Y98 and R52 (*27*). On the basis of the high-resolution NMR structure of dark-state PYP, the interaction between R52 and Y98 would occur through a cation$-\pi$ interaction between the guanidinium group of R52 and the aromatic ring of Y98 (*22*), instead of with the carbonyl oxygen atom of Y98 as observed in the crystal structure. It was thought that a Y to Q mutation would lead to a loss of interaction between the $\alpha3-\alpha4$ and the $\beta4-\beta5$ loops, creating a more flexible conformation of the $\beta4-\beta5$ loop which could affect the recovery kinetics. However, the X-ray structure of Y98Q shows that Q99 has moved in to fill in the gap after the Q98 movement and the interaction between the $\alpha3-\alpha4$ loop and the $\beta4-\beta5$ loop is restored through the interaction of Q99 and the repositioned R52. Although the $\beta4-\beta5$ loop is clearly distorted in Y98Q compared to WT PYP, there is no obvious difference in flexibility. Apparently, there is a strong need for the protein to maintain a stable interaction between the $\alpha3-\alpha4$ loop and the $\beta4-\beta5$ loop, since it occurs at the expense of a serious distortion of the $\beta4-\beta5$ loop with significant consequences on the photocycle.

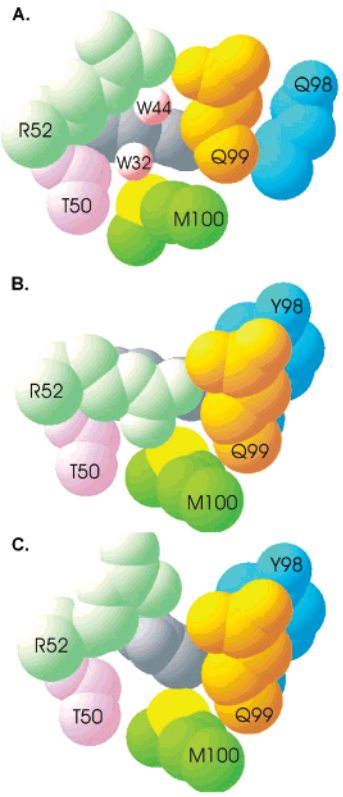

FIGURE 6: Space-filling presentation of the area around the chromophore (in gray). Panel A is the Y98Q structure showing the opening from the solvent to the chromophore, filled in by two water molecules. Note the similarity with panel C, which shows the conformation in the presumed I_2 state (*21*). The WT dark state structure, where R52 shields the chromophore from solvent, is shown in panel B.

It had been shown that R52 shields the chromophore from solvent in dark state WT PYP, but moves away during I_2 formation and provides solvent access to the *cis* chromophore (*21*). Through its rotation in the Y98Q mutant, R52 has taken on a position that resembles its position in the I_2 state and has thereby created an opening from the solvent to the chromophore. Figure 6 illustrates the opening from the solvent in both the Y98Q dark state and the WT I_2 with a space-filling representation. Two water molecules have filled the space and in doing so have come in close proximity to the phenolic ring of the chromophore. These polar water molecules will increase the dielectric constant of the chromophore environment, which suggests an explanation for the red shift of the fluorescence emission maxima we observed with the Y98Q mutant (4 nm) and the P68A mutant (7 nm) in terms of solvent polarity. The requirement for a red-shifting polarity probe is that the permanent electric dipole moment in the excited state is larger than in the ground state (*36*), which is indeed the case for the *p*-hydroxycinnamoyl chromophore of PYP (*41*). We conclude that the chromophore emission wavelength serves as a sensitive polarity probe. The guanidinium group of R52 is thought to interact with the phenolic oxygen of the *cis* chromophore in the I_2 state, which implies that, in the Y98Q mutant, R52 will have to rotate around its C$\gamma-$Cδ bond and break its hydrogen

bonds with Q99 and Q56 before it can interact with the phenolic oxygen of the chromophore. This is different from its movement during WT I_2 formation and could partially explain the slower formation of I_2 we observed in Y98Q (*27*). It is not known what drives the movement of R52 during the photocycle, but since the ground state conformation of R52 is different in Y98Q, it might not be as inclined to move.

The R52A substitution causes a 6-fold decrease in the recovery rate (*23*). Since a repositioning of both M100 and R52 occurs in the Y98Q mutant, we investigated whether an R52 substitution is also linked to M100 by investigating the R52A/M100A mutant. Although the absorption maximum did not differ from WT, we found that there is a significant effect on recovery kinetics of the R52A substitution in addition to the M100A mutation. This indicates that the effect of R52 on the photocycle is distinct from the catalysis of reisomerization by M100. The recovery kinetics of R52A/M100A shows sigmoidal pH dependence similar to M100A; however, the recovery is about 2 times slower at pH 7 and about 2 times faster at pH 10. It had previously been suggested that the pK_a of 7 in M100 mutants could be ascribed to the improbable ionization of the surface-exposed R52 (*25*). Our results with the R52A/M100A mutant now clearly show that R52 is not responsible for the pK_a of 7 since that pK_a is still present after the R52A mutation. The two pK_a values for WT recovery have been attributed to ionization of E46 (pK_a 6.4) and of the chromophore in the bleached state (pK_a 9.4; *42*). Since these values are very similar to the pK_a values of M100 and R52A/M100A, we believe that our original explanation for the pK_a values, that is, E46 and the chromophore, of WT and mutants is also correct in these cases. In addition, the R52A/M100A recovery has a third pK_a value of 7.6, which was not observed in WT or M100A. This pK_a indicates that there are additional electrostatic factors in the protein that facilitate isomerization; however, further mutagenesis and kinetic studies will be necessary to identify the nature of these interactions. We can conclude that, although the reisomerization of the chromophore during recovery is clearly still the rate-limiting step in the R52A/M100A mutant, there is an additional effect of the R52A substitution, which was not observed in Y98Q/M100A.

It has been suggested that the path to chromophore isomerization is ensured by a gateway formed by C9 of the chromophore and the *pro-R* Cβ hydrogen of Y98 (*10*). This gateway has ratchet-like properties, which prevent the chromophore thioester oxygen from flipping back to its original stereochemistry, and therefore drives the progression of the photocycle (*10*). Combined motions of Y98, P68, and the chromophore are thought to be necessary to open and close this gateway. We can therefore expect that a mutation at position 98 will affect the properties of the gateway to a certain degree. We find that, in the Y98Q structure, there is a significant opening of this gateway (about 1 Å) due to the movement of residue 98 and a subtle repositioning of P68 and the chromophore. The fluorescence in P68A was increased substantially (up to 4-fold higher than WT). The P68 and Y98 mutant results indicate that disrupting the gateway has a significant effect on the fluorescence yield and possibly on the initiation of the photocycle. On the basis of our structural data we find it plausible that the opening of the gateway allows the chromophore to obtain a more planar conformation which is otherwise prevented by the steric hindrance between the chromophore carbonyl oxygen and the Cβ of Y98. As explained above, this could significantly increase the fluorescence. The opening of the gateway also implies that the ratchet-like properties are lost. If the chromophore returns to the *trans* position readily, there will be less initiation of the photocycle, resulting in a lower quantum efficiency. The quantum efficiency for the photocycle of WT PYP has been reported to be ~0.6 (*43*), although independent reports have determined it to be lower (~0.35; *44*). The quantum efficiency of P68A is about the same (0.4; *45*). The higher degree of fluorescence found in our study and a possibly slightly lower quantum yield for the photocycle indicate that a change in the gateway changes the initiation of the photocycle. On the other hand, the recovery kinetics of P68A are similar to those of WT PYP. This suggests that the gateway itself does not play a rate-limiting role in the recovery of PYP from the signaling state to the ground state. This is in agreement with the structural data from the presumed I_2 state of WT PYP (*21*), where the chromophore has obtained its *cis* conformation by flipping the aromatic ring toward the solvent and, concomitantly, the chromophore carbonyl is already back in a ground state-like position in the I_2 state.

ACKNOWLEDGMENT

We thank Elsa Chan for technical support and the laboratory of Dr. Nancy Horton (University of Arizona) for the use of their PC1 photon counting spectrofluorometer. Furthermore, we thank the EMBL Hamburg Outstation (supported by the Research Infrastructure Action under the EU-FP6 "Structuring the European Research Area Specific Programme", Contract RII3-CT-2004-506008) for synchrotron facilities and help with data collection.

REFERENCES

1. Meyer, T. E., Yakali, E., Cusanovich, M. A., and Tollin, G. (1987) Properties of a water-soluble, yellow protein isolated from a halophilic phototrophic bacterium that has photochemical activity analogous to sensory rhodopsin, *Biochemistry 26*, 418−423.
2. Cusanovich, M. A., and Meyer, T. E. (2003) Photoactive yellow protein: A prototypic PAS domain sensory protein and development of a common signaling mechanism, *Biochemistry 42*, 4759−4770.
3. Meyer, T. E. (1985) Isolation and characterization of soluble cytochromes, ferredoxins and other chromophoric proteins from the halophilic phototrophic bacterium *Ectothiorhodospira halophila*, *Biochim. Biophys. Acta 806*, 175−183.
4. Kyndt, J. A., Meyer, T. E., and Cusanovich, M. A. (2004) Photoactive yellow protein, bacteriophytochrome, and sensory rhodopsin in purple phototrophic bacteria, *Photochem. Photobiol. Sci. 3*, 519−530.
5. Jiang, Z. Y., Swem, L. R., Rushing, B. G., Devanathan, S., Tollin, G., and Bauer, C. E. (1999) Bacterial photoreceptor with similarity to photoactive yellow protein and plant phytochromes, *Science 285*, 406−409.
6. Kyndt, J. A., Fitch, J. C., Meyer, T. E., and Cusanovich, M. A. (2005) *Thermochromatium tepidum* photoactive yellow protein/bacteriophytochrome/diguanulate cyclase: Characterization of the PYP domain, *Biochemistry 44*, 4755−4764.
7. Haker, A., Hendriks, J., Gensch, T., Hellingwerf, K., and Crielaard, W. (2000) Isolation, reconstitution and functional characterization of the *Rhodobacter sphaeroides* photoactive yellow protein, *FEBS Lett. 486*, 52−56.
8. Kyndt, J. A., Hurley, J. K., Devreese, B., Meyer, T. E., Cusanovich, M. A., Tollin, G., and Van Beeumen, J. J. (2004) *Rhodobacter*

capsulatus photoactive yellow protein: Genetic context, spectral and kinetics characterization, and mutagenesis, *Biochemistry 43*, 1808−1820.

9. Wise, K. J., Gillespie, N. B., Stuart, J. A., Krebs, M. P., and Birge, R. R. (2002) Optimization of bacteriorhodopsin for bioelectronic devices, *Trends Biotechnol. 20*, 387−394.
10. Getzoff, E. D., Gutwin, K. N., and Genick, U. K. (2003) Anticipatory active-site motions and chromophore distortion prime photoreceptor PYP for light activation, *Nat. Struct. Biol. 10*, 663−668.
11. Ujj, L., Devanathan, S., Meyer, T. E., Cusanovich, M. A., Tollin, G., and Atkinson, G. H. (1998) New photocycle intermediates in the photoactive yellow protein from *Ectothiorhodospira halophila*: Picosecond transient absorption spectroscopy, *Biophys. J. 75*, 406−412.
12. Devanathan, S., Pacheco, A., Ujj, L., Cusanovich, M., Tollin, G., Lin, S., and Woodbury, N. (1999) Femtosecond spectroscopic observations of initial intermediates in the photocycle of the photoactive yellow protein from *Ectothiorhodospira halophila*, *Biophys. J. 77*, 1017−1023.
13. Borucki, B., Devanathan, S., Otto, H., Cusanovich, M. A., Tollin, G., and Heyn, M. P. (2002) Kinetics of proton uptake and dye binding by photoactive yellow protein in WT and in the E46Q and E46A mutants, *Biochemistry 41*, 10026−10037.
14. Borucki, B., Otto, H., Joshi, C. P., Cusanovich, M. A., Devanathan, S., Tollin, G., and Heyn, M. P. (2003) pH dependence of the photocycle kinetics of the E46Q mutant of photoactive yellow protein: Protonation equilibrium between I_1 and I_2 intermediates, chromophore deprotonation by hydroxyl uptake, and protonation relaxation of the dark state, *Biochemistry 42*, 8780−8790.
15. Xie, A., Kelemen, L., Hendriks, J., White, B. J., Hellingwerf, K. J., and Hoff, W. D. (2001) Formation of a new buried charge drives a large-amplitude protein quake in photoreceptor activation, *Biochemistry 40*, 1510−1517.
16. Joshi, C. P., Borucki, B., Otto, H., Meyer, T. E., Cusanovich, M. A., and Heyn, M. P. (2005) Photoreversal kinetics of the I_1 and I_2 intermediates in the photocycle of photoactive yellow protein by double flash experiments with variable time delay, *Biochemistry 44*, 656−665.
17. Otto, H., Hoersch, D., Meyer, T. E., Cusanovich, M. A., and Heyn, M. P. (2005) Time-resolved single tryptophan fluorescence in photoactive yellow protein monitors changes in the chromophore structure during the photocycle via energy transfer, *Biochemistry 44*, 16804−16816.
18. Shimizu, N., Imamoto, Y., Harigai, M., Kamikubo, H., Yamazaki, Y., and Kataoka, M. (2006) pH-dependent equilibrium between long lived near-UV intermediates of photoactive yellow protein, *J. Biol. Chem. 281*, 4318−4325.
19. Borgstahl, G. E. O., Williams, D. R., and Getzoff, E. D. (1995) 1.4 Å structure of photoactive yellow protein, a cytosolic photoreceptor: Unusual fold, active site, and chromophore, *Biochemistry 34*, 6278−6287.
20. Taylor, B. L., and Zhulin, I. B. (1999) PAS domains: Internal sensors of oxygen, redox potential, and light, *Microbiol. Mol. Biol. Rev. 63*, 479−506.
21. Genick, U. K., Borgstahl, G. E. O., Ng, K., Ren, Z., Pradervand, C., Burke, P. M., Srajer, V., Teng, T.-Y., Schildkamp, W., McRee, D. E., Moffat, K., and Getzoff, E. D. (1997) Structure of a protein photocycle intermediate by millisecond time-resolved crystallography, *Science 275*, 1471−1475.
22. Düx, P., Rubinstenn, G., Vuister, G. W., Boelens, R., Mulder, F. A. A., Hård, K., Hoff, W. D., Kroon, A. R., Crielaard, W., Hellingwerf, K. J., and Kaptein, R. (1998) Solution structure and backbone dynamics of the photoactive yellow protein, *Biochemistry 37*, 12689−12699.
23. Genick, U. K., Devanathan, S., Meyer, T. E., Canestrelli, I. L., Williams, E., Cusanovich, M. A., Tollin, G., and Getzoff, E. D. (1997) Active site mutants implicate key residues for control of color and light cycle kinetics of photoactive yellow protein, *Biochemistry 36*, 8−14.
24. Devanathan, S., Genick, U. K., Canestrelli, I. L., Meyer, T. E., Cusanovich, M. A., Getzoff, E. D., and Tollin, G. (1998) New insights into the photocycle of *Ectothiorhodospira halophila* photoactive yellow protein: Photorecovery of the long-lived photobleached intermediate in the Met100Ala mutant, *Biochemistry 37*, 11563−11568.
25. Kumauchi, M., Hamada, N., Sasaki, J., and Tokunaga, F. (2002) A role of methionine100 in facilitating PYP_M decay process in the photocycle of photoactive yellow protein, *J. Biochem. 132*, 205−210.
26. Rajagopal, S., and Moffat, K. (2003) Crystal structure of a photoactive yellow protein from a sensor histidine kinase: Conformational variability and signal transduction, *Proc. Natl. Acad. Sci. U.S.A. 100*, 1649−1654.
27. Borucki, B., Kyndt, J. A., Joshi, C. P., Otto, H., Meyer, T. E., Cusanovich, M. A., and Heyn, M. P. (2005) Effect of salt and pH on the activation of photoactive yellow protein and gateway mutants Y98Q and Y98F, *Biochemistry 44*, 13650−13663.
28. Kyndt, J. A., Vanrobaeys, F., Fitch, J. C., Devreese, B. V., Meyer, T. E., Cusanovich, M. A., and Van Beeumen, J. J. (2003) Heterologous production of *Halorhodospira halophila* holophotoactive yellow protein through tandem expression of the postulated biosynthetic genes, *Biochemistry 42*, 965−970.
29. Otwinowski, Z. and Minor, W. (1997) Processing of X-ray diffraction data collected in oscillation mode, *Methods Enzymol. 276*, 307−326.
30. Storoni, L. C., McCoy, A. J., and Read, R. J. (2004) Likelihood-enhanced fast rotation functions, *Acta Crystallogr. D60*, 432−438.
31. Brunger, A. T., Adams, P. D., Clore, G. M., DeLano, W. L., Gros, P., Grosse-Kunstleve, R. W., Jiang, J. S., Kuszewski, J., Nilges, M., Pannu, N. S., Read, R. J., Rice, L. M., Simonson, T., and Warren, G. L. (1998) Crystallography & NMR system: A new software suite for macromolecular structure determination, *Acta Crystallogr., Sect. D: Biol. Crystallogr. 54*, 905−921.
32. Lovell, S. C., Davis, I. W., Arendall, W. B., III, de Bakker, P. I. W., Word, J. M., Prisant, M. J., Richardson, J. S., and Richardson, D. C. (2003) Structure validation by Cα geometry: ϕ, ψ, and Cβ deviation, *Proteins: Struct., Funct., Genet. 50*, 437−450.
33. Simondsen, R. P., and Tollin, G. (1983) Transient kinetics of redox reactions of flavodoxin: Effects of chemical modification of the flavin mononucleotide prosthetic group on the dynamics of intermediate complex formation and electron transfer, *Biochemistry 22*, 3008−3016.
34. Anderson, S., Crosson, S., and Moffat, K. (2004) Short hydrogen bonds in photoactive yellow protein, *Acta Crystallogr. D60*, 1008−1016.
35. Meyer, T. E., Tollin, G., Causgrove, T. P., Cheng, P., and Blankenship, R. E. (1991) Picosecond decay kinetics and quantum yield of fluorescence of the photoactive yellow protein from the halophilic purple phototrophic bacterium, *Ectothiorhodospira halophila*, *Biophys. J. 59*, 988−991.
36. Lackowicz, J. R. (2006) *Principles of Fluorescence Spectroscopy*, 3rd ed., Springer Publishing, New York.
37. Morishita, T., Harigai, M., Yamazaki, Y., Kamikubo, H., Kataoka, M., and Imamoto, Y. (2006) Array of aromatic amino acid side chains located near the chromophore of photoactive yellow protein, *Photochem. Photobiol.* (Epub 6/1/06).
38. Brudler, R., Meyer, T. E., Genick, U. K., Devanathan, S., Woo, T. T., Millar, D. P., Gerwert, K., Cusanovich, M. A., Tollin, G., and Getzoff, E. D. (2000) Coupling of hydrogen bonding to chromophore conformation and function in photoactive yellow protein, *Biochemistry 39*, 13478−13486.
39. Quillin, M. L., Anstrom, D. M., Shu, X., O'Leary, S., Kallio, K., Chudakov, D. M., and Remington, S. J. (2005) Kindling fluorescent protein from *Anemonia sulcata*: Dark-state structure at 1.38 Å resolution, *Biochemistry 44*, 5774−5787.
40. Harigai, M., Kataoka, M., and Imamoto, Y. (2006) A single CH/π weak hydrogen bond governs stability and the photocycle of the photoactive yellow protein, *J. Am. Chem. Soc. 128*, 10646−10647.
41. Premvardhan, L. L., van der Horst, M. A., Hellingwerf, K. J., and van Grondelle, R. (2003) Stark spectroscopy on photoactive yellow protein, E46Q, and a nonisomerizing derivative, probes photoinduced charge motion, *Biophys. J. 84*, 3226−3239.
42. Meyer, T. E., Devanathan, S., Woo, T., Getzoff, E. D., Tollin, G., and Cusanovich, M. A. (2003) Site specific mutations provide new insights into the origin of pH effects and alternative spectral forms in the photoactive yellow protein from *Ectothiorhodospira halophila*, *Biochemistry 42*, 3319−3325.
43. Meyer, T. E., Tollin, G., Hazzard, J. H., and Cusanovich, M. A. (1989) Photoactive yellow protein from the purple phototrophic bacterium, *Ectothiorhodospira halophila*, *Biophys. J. 56*, 559−564.
44. Van Brederode, M. E., Gensch, T., Hoff, W. D., Hellingwerf, K. J., and Braslavsky, S. E. (1995) Photoinduced volume change and

energy storage associated with the early transformations of the photoactive yellow protein from *Ectothiorhodospira halophila*, *Biophys. J. 68*, 1101−1109.
45. Takeshita, K., Imamoto, Y., Kataoka, M., Mihara, K., Tokunaga, F., and Terazima, M. (2002) Structural change of site-directed mutants of PYP: New dynamics during pR state, *Biophys. J. 83*, 1567−1577.
46. Bruns, C. M., Hubatsch, I., Ridderström, M., Mannervik, B., and Tainer, J. A. (1999) Human glutathione transferase A4-4. Crystal structures and mutagenesis reveal the basis of high catalytic efficiency with toxic lipid peroxidation products, *J. Mol. Biol. 288*, 427−439.

BI061867Y